Non Reflecting Boundary Conditions For Reacting Flows

Robert Prosser

Department of Mechanical, Aerospace and Civil Engineering, University of Manchester, Manchester M60 1QD

Tel: +44 (0)161 200 3716

E-mail: robert.prosser@manchester.ac.uk

keywords : characteristics, turbulence, boundary conditions

abstract

In this paper we explore the specification of time dependent boundary conditions suitable for the simulation of low Mach number reacting flows. The standard treatments used to date are based on the method of characteristics, and essentially set to zero the incoming characteristics; this practise has been shown to have deleterious effects on the flow evolution. The new approach, while still based on the method of characteristics, circumvents this problem through the application of a double expansion in terms of an appropriately defined Mach number. In the method, a low Mach number expansion of the dependent variables is coupled to a two-length scale decomposition. Through the double expansion, it is possible to separate inertial events (i.e. those moving at the local convection velocity) from acoustic events (those moving at the local sound speed). The paper highlights why previous treatments have encountered difficulties in turbulent flows, and provides a method by which heat release effects can be incorporated into a non-reflecting boundary condition framework. The accuracy of the method is demonstrated using a curved stagnating flame, in which the reaction zone crosses the boundary.

1 Introduction

The accuracy of a compressible flow calculation is strongly dependent on the choice of boundary conditions supplementing the governing equations. If the flow domain is open, the boundary conditions' purpose is to provide a truncation of the physical problem to reduce the computational burden. If the flow

exiting the domain is turbulent, then the specification of the boundary conditions is challenging due to the existence of a spectrum of non-stationary length and time scales. On a purely practical level, specifying the flow variables for a turbulent flow appears almost impossible, yet incorrect boundary conditions can alter significantly the evolution of flow properties such as vorticity [1] . This paper describes recent developments designed to address this issue.

Considerable effort has been expended in the development of time dependent boundary conditions. In the review by Tsynkov [2], most artificial boundary conditions are classified according to two categories: global methods and local methods. The former approach has the advantage of being accurate and robust, but is not straightforward to implement in problems with complex geometries or reacting flows. Local methods have seen considerable development in recent years and, although they were originally designed for the linearized Euler system [3–7], extensions to other flows have also been discussed. These extensions are largely based around the **N**avier-**S**tokes **C**haracteristic **B**oundary **C**onditions (NSCBC) and the **L**ocal **O**ne **D**imensional **I**nviscid (LODI) approaches developed by Poinsot et al. [8], and have sought to incorporate viscous and reacting effects [9–12].

In the analysis of Giles [13], the LODI approach is seen to be a first order approximation to the null vectors associated with the dispersion relation derived from the linearized Euler system. The approach is known to be inadequate when the flow contains perturbations that are not driven purely by acoustic effects [13–15], and produces spurious pressure reflections. This effect has been observed by Grinstein [1], who noted that the application of one dimensional non-reflecting boundary conditions at an outflow can have significant effects on the vorticity distribution associated with free shear layers. The higher order asymptotic expansions developed by Giles to address this problem do not appear to provide significant improvements [13].

Colonius et al [14] have attempted to extend the range of the characteristics based boundary conditions by treating the flow as a perturbation around a reference state that is in some sense 'near' to the actual flow evolution. They point out that such a reference flow need not satisfy the Navier-Stokes equations, but is rather an artifact designed to improve the accuracy of the linearization used to develop the boundary conditions. Even disregarding the difficulties of specifying an appropriate base flow in complex geometries, the results they presented were not significantly improved by this practise. We will demonstrate in the body of this paper that by linearizing about a base state defined in terms of an *inertial divergence*, their goal of an optimal reference state can be derived for all manner of flows without recourse to ad-hoc assumptions.

In earlier work, we described how to apply the method to inviscid turbulence

at low Mach number [16] and more recently we extended the treatment to hot flows with molecular transport [17]. This paper completes the analysis by examining boundary conditions for problems with significant enthalpy transport and chemical reaction effects. The boundary condition is tested using a curved flame, with a reaction zone that crosses the computational boundary.

Section 2 reviews the method-of-characteristics approach, and introduces the coupled low Mach number expansion employed. The test problem, details of the numerical code employed and some preliminary results are detailed in section 3. Conclusions and directions for additional work are discussed in section 4.

2 The method of Characteristics

2.1 Governing equations

We consider the specification of time dependent outflow conditions for a two dimensional reacting flow problem comprising N_s species. The inflow problem has already been discussed elsewhere [16] and (provided the reaction zone does not propagate into the inflow boundary) is usually easier to specify than the outflow. The restriction of the discussion to two dimensional problems is purely for ease of presentation. We adopt a method of characteristics approach [3], in which the governing equations in two dimensions are expressed as

$$\frac{\partial}{\partial t}\left(\mathbf{U}\right) + \mathbf{S}_{\alpha}^{-1}\mathbf{L}_{\alpha}\frac{\partial}{\partial \widetilde{x}_{\alpha}}\left(\mathbf{U}\right) + \sum_{\substack{i=1 \\ i\neq\alpha}}^{2}\mathbf{P}^{-1}\left(\mathbf{F}_{i}\right)_{\mathbf{U}}\frac{\partial}{\partial \widetilde{x}_{i}}\left(\mathbf{U}\right) = \mathbf{P}^{-1}\mathbf{C}. \qquad (1)$$

In equation 1, $\mathbf{L}_{\alpha} = \{L_1, L_2, \ldots, L_{N_s+4}\}^T$ is the so-called vector of *characteristic wave amplitude variations* (or *amplitudes* hereafter), $\mathbf{U}$ is a (non-unique) vector of primitive variables, $\mathbf{P}$ is a transformation matrix relating primitive and conserved quantities, $\mathbf{F}_i$ is the flux vector, and $\mathbf{S}_{\alpha}$ is the matrix of left eigenvalues of $\mathbf{P}^{-1}\left(\mathbf{F}_{\alpha}\right)_{\mathbf{U}}$. There is no summation over Greek indices. The amplitude vector is associated with $N_s + 4$ eigenvalues: a left-going and a right-going 'acoustic' or non-linear amplitude [18] (propagating with speeds $u - a$ and $u + a$, respectively), and $N_s + 2$ degenerate eigenvectors with propagation speed u representing convective transport. A non reflecting outflow is traditionally obtained by setting to zero all of those amplitudes that are incoming at the outflow. The success of this approach relies largely on the linearization of the underlying flow field about some suitably defined quiescent state. If the flow is not well approximated by this state (i.e. if the flow is turbulent), then the boundary conditions produce very large spurious pressure

field oscillations [16].

For definiteness, we consider a consider a square domain, whose boundaries are aligned normal to the x and y axes. The inflow will be taken to be at $x = 0$ and the outflow will be assumed to be at $x = 1$ (dimensionless quantities are assumed throughout the paper, unless otherwise stated). Spanwise periodicity will be assumed for the following discussion, although in the non-periodic case they can be treated in the same manner as discussed below.

The only incoming amplitude at $x = 1$ will be that associated with the $(u - a)$ eigenvalue; we will assume L_1 is associated with this eigenvalue. We take L_4 to be associated with the $(u + a)$ eigenvalue, and the remaining amplitudes to be associated with the degenerate eigenvalue. This nomenclature is adopted as it is easier to extend the treatment to an arbitrary number of chemical species; $L_5, L_6, \ldots L_{N_s+4}$ represent species mass fraction transport.

2.2 Low Mach number expansions

We apply a low Mach number expansion coupled with a two scale decomposition to the amplitudes associated with equation 1. The dependent variables are thus expressed as (in the case of pressure, say)

$$p = p^{(0)} + Mp^{(1)} + M^2 p^{(2)} + O\left(M^3\right)$$

where the bracketed superscript refers to the index of the term in the expansion and M refers to the flow Mach number. The second decomposition separates the flow physics on to two distinct length scales; the length scales $\mathbf{x} = (x, y)^T$ are interpreted as evolving via inertial (slow moving) processes, while physical processes defined on length scales $\boldsymbol{\eta} = (\xi, \eta)^T = (Mx, My)^T$ are associated with acoustic phenomena. This terminology is driven by the role of the pressure at leading, first and second orders in the Mach number [19]. The derivatives appearing in the amplitude definitions and the transport equations can thus be expressed as (in the case of the $x-$ direction)

$$\left.\frac{\partial}{\partial \widetilde{x}}\right|_{M,t} = \frac{\partial}{\partial x} + M\frac{\partial}{\partial \xi}.$$

Applying this decomposition to the incoming and outgoing acoustic amplitudes, we find

$$
\begin{aligned}
L_1 &= L_1^{(0)} + M L_1^{(1)} + \ldots \\
&= \frac{1}{2\rho^{(0)} c_p} \left(\gamma p^{(0)} \frac{\partial u^{(0)}}{\partial x} + M \left(\gamma p^{(0)} \left(\frac{\partial u^{(0)}}{\partial \xi} + \frac{\partial u^{(1)}}{\partial x} + \frac{\partial u^{(0)}}{\partial x} \left(\frac{p^{(1)}}{p^{(0)}} - \frac{\rho^{(1)}}{\rho^{(0)}} \right) \right) \right. \right. \\
&\quad \left. \left. - \sqrt{\frac{\gamma p^{(0)}}{\rho^{(0)}}} \left\{ \frac{\partial p^{(1)}}{\partial \xi} + \frac{\partial p^{(2)}}{\partial x} + \rho^{(0)} u^{(0)} \frac{\partial u^{(0)}}{\partial x} \right\} \right) \right) + O\left(M^2\right) \qquad (2) \\
L_4 &= L_4^{(0)} + M L_4^{(1)} + \ldots \\
&= \frac{1}{2\rho^{(0)} c_p} \left(\gamma p^{(0)} \frac{\partial u^{(0)}}{\partial x} + M \left(\gamma p^{(0)} \left(\frac{\partial u^{(0)}}{\partial \xi} + \frac{\partial u^{(1)}}{\partial x} + \frac{\partial u^{(0)}}{\partial x} \left(\frac{p^{(1)}}{p^{(0)}} - \frac{\rho^{(1)}}{\rho^{(0)}} \right) \right) \right. \right. \\
&\quad \left. \left. + \sqrt{\frac{\gamma p^{(0)}}{\rho^{(0)}}} \left\{ \frac{\partial p^{(1)}}{\partial \xi} + \frac{\partial p^{(2)}}{\partial x} + \rho^{(0)} u^{(0)} \frac{\partial u^{(0)}}{\partial x} \right\} \right) \right) + O\left(M^2\right). \qquad (3)
\end{aligned}
$$

The acoustic waves are described in each of the above definitions by the terms

$$
M \left(\gamma p^{(0)} \frac{\partial u^{(0)}}{\partial \xi} \pm \sqrt{\frac{\gamma p^{(0)}}{\rho^{(0)}}} \frac{\partial p^{(1)}}{\partial \xi} \right)
$$

where the sign indicates a left going or right-going wave. The standard non-reflecting treatment of Hedstrom [5] specifies

$$
\gamma p \frac{\partial u}{\partial x} \pm \sqrt{\frac{\gamma p}{\rho}} \frac{\partial p}{\partial x} = 0
$$

which, by comparison to equations 2 and 3 can be seen to discard incorrectly both the thermodynamic behaviour (leading order) and the inertial behaviour ($O\left(M^2\right)$).

The LODI/NSCBC prescriptions of Poinsot et al [8,11,10], balance L_1 and L_4 such that the resulting formulation exactly satisfies some pre-specified condition (such as steady behaviour at the boundary). In so doing, their approach incorrectly matches the outgoing acoustic wave with an incoming one yielding a fully reflective boundary condition [16]. We observe that the LODI/NSCBC treatment provides good boundary conditions if the flow is quiescent; in that case the leading order and $O\left(M^2\right)$ terms vanish from the expansions in equations 2 and 3, and the Hedstrom condition is correctly applied only to the acoustic components of the flow. In the general case, the leading order velocity gradient is non-zero, and we require some means of estimating its value. Once we have this estimate, we can linearize the flow around this non-zero dilatation. By so doing, we can guarantee to apply the non-reflecting condition only to the acoustic components of the flow. In previous work, we have shown that such a linearization can be achieved both for cold flows [16] and for thermally conductive flows [17]. We begin by defining the numerical divergence

as

$$\Delta = \Delta^{(0)} + M\Delta^{(1)} + O\left(M^2\right) = \frac{\partial u}{\partial \widetilde{x}} + \frac{\partial u}{\partial \widetilde{y}},$$

where the velocity gradients are calculated using some numerical scheme. For any type of flow (i.e. hot or cold), a convective non-reflecting outflow boundary condition can then be shown to be [17]

$$L_1 = L_4 + T\sqrt{\frac{\rho}{\gamma p}}\left(v\frac{\partial u}{\partial y} - u_b\frac{\partial u}{\partial x}\right) - (\gamma - 1)\,T\left(\Delta^{(1)}\right), \tag{4}$$

where u_b is used to denote the bulk velocity at the outflow. Equation 4 can be used without the $\Delta^{(1)}$ term, in which case the boundary condition becomes fully reflective.

The problem of boundary condition specification then devolves to that of estimating the acoustic dilatation in a general flow. If the flow is cold and at low Mach number, then it is straightforward to show that the velocity field is solenoidal to leading order; any departure from solenoidal behaviour observed in the simulation must be acoustic in origin, i.e.

$$\Delta \simeq M\Delta^{(1)}.$$

Such an identity does not hold in hot, reactive flows, where divergence effects can emerge as a result of conduction, enthalpy transport or reaction. In this latter case, guidance in the determination of $\Delta^{(0)}$ can be obtained from the pressure transport equation, which, in dimensional form is written as [20]

$$\begin{aligned}\frac{Dp}{Dt} + \gamma p\nabla\cdot\mathbf{u} = (\gamma-1)\left(\tau : \nabla\mathbf{u} + \nabla\cdot(\lambda\nabla T) + \sum_{\alpha=1}^{N_s}\nabla\cdot(h_\alpha\rho D_\alpha\nabla Y_\alpha)\right)\\ + \sum_{\alpha=1}^{N_s}\left(\omega_\alpha + \nabla\cdot(\rho D_\alpha\nabla Y_\alpha)\right)(h_\alpha - \gamma e_\alpha).\end{aligned} \tag{5}$$

By applying the low Mach number expansion and two scale decomposition to the dimensionless form of equation 5 it is straightforward to show that

$$\begin{aligned}\gamma p^{(0)}\nabla_x\cdot u^{(0)} = (\gamma-1)\left(\nabla_x\cdot\left(\lambda\nabla_x T^{(0)}\right) + \sum_{\alpha=1}^{N_s}\nabla_x\cdot\left(h_\alpha^{(0)}\rho D_\alpha\nabla_x Y_\alpha\right)\right)\\ + \sum_{\alpha=1}^{N_s}\left(\omega_\alpha^{(0)} + \nabla_x\cdot(\rho D_\alpha\nabla Y_\alpha)\right)\left(h_\alpha^{(0)} - \gamma e_\alpha^{(0)}\right).\end{aligned} \tag{6}$$

In equation 6, we have assumed that the thermal conduction and mass diffusivity are constant; this is not necessary, but is used for notational convenience. We observe that species mass fraction gradients are leading order effects alone, and this explains why they are not indexed in the same way as other terms.

In the absence of chemical reaction, equation 6 reverts to the conducting case described in [17]; in the absence of conduction, $\nabla_x \cdot u^{(0)} = 0$ and the flow reverts to the cold turbulent flows considered in [16].

In summary, we specify the outflow boundary condition on L_1 via equation 4, with

$$\Delta^{(1)} = \Delta - M\Delta^{(0)},$$

where Δ is the numerically calculated divergence, and $\Delta^{(0)}$ is given by equation 6. We note that this approach is identical to that derived in [16], and differs only in the expression for $\Delta^{(0)}$.

3 Results

3.1 Test configuration

We have tested the boundary condition (eq. 4) via the simulation of a curved stagnating flame. The initial conditions are estimated using potential flow theory. A point source is placed far to the right of the outflow, and a planar flow is assumed at $x = -\infty$. By controlling the strength and position of the source, flames with different curvatures and strain rates can be simulated. The flow is not inviscid, however, and both reaction and transport effects cause the solution to move rapidly away from the initial conditions through the production of a large transient pressure field. This leaves via the non-reflecting conditions. The new non-reflective outflows are specified on the spanwise boundaries. 'Fixed' conditions are specified on the $x-$boundaries, by which we understand that the inertial component of the velocity does not change on these boundaries—they are, however, still non-reflecting. The flame crosses the computational boundary at an oblique angle.

3.2 Code configuration

The code used to test the new boundary conditions has been developed in-house at the University of Manchester. The code is based on a finite difference approach, and has been tested against a number of benchmark problems in order to accommodate the validation steps recommended by Roache [21,22]. The software is a general compressible flow solver; it is able to work on either parallel or serial architectures and can, if required, deal with arbitrary reaction mechanisms and molecular transport. Time integration is achieved via a minimal storage, 3^{rd} order Runge-Kutta method taken from the family described by Wray [23]. The code has a modular structure, and any one of a

number of different numerical methods can be employed to suit a particular application. For the work described in this paper, the spatial discretization is performed using explicit 4^{th} order schemes in both directions.

3.3 Chemistry

In order to match a parallel asymptotic study on plane flames, a square domain of side approximately 1mm is used, with 128 grid points used in each spatial direction. The flame structure is over-resolved; this is a conscious decision to ensure that instabilities emerging from the solution (if any) are due to the new boundary conditions, and not to under-resolving the reaction zone. The flame has a single step chemistry, exemplified by

$$Reactants \rightarrow Products,$$

with a reaction rate given by

$$\omega = \rho B^* (1-c) \exp\left(\frac{-\beta (1-c)}{1-\alpha (1-c)}\right),$$

where $B^* = 285 \times 10^3 s^{-1}$, the Zeldovitch number $\beta = 6$, and $\alpha = 0.8$ (corresponding to a heat release of 4). This leads to a product temperature of $1500K$. Molecular transport is handled by the joint assumptions of constant Lewis number and a constant Prandtl number. The thermal conductivity is given by [24]

$$\lambda = 2.58 \times 10^5 c_p,$$

where the temperature dependence of λ has been suppressed. The leading order divergence term is estimated in dimensional form using equation 6;

$$\nabla_x \cdot u^{(0)} \simeq \frac{1}{\gamma p}\left((\gamma-1)\left(\nabla\cdot(\lambda\nabla T) + \sum_{\alpha=1}^{2} \nabla\cdot(h_\alpha \rho D_\alpha \nabla Y_\alpha)\right) + \sum_{\alpha=1}^{2} (\omega_\alpha + \nabla\cdot(\rho D_\alpha \nabla Y_\alpha))(h_\alpha - \gamma e_\alpha)\right), \quad (7)$$

where all spatial gradients are calculated numerically.

3.4 Curved flame results

Figure 1 shows the velocity vectors associated with the curved flame front. The latter is shown as the family of curved contours. We observe that the

flame crosses the boundary with no apparent ill effects. The curvature appears to produce a lensing effect which, in turn, will increase the curvature of the flame in the absence of other effects. The lensing is also responsible for the entrainment behaviour of the spanwise boundaries—these act as part inflow and part outflow.

The pressure field associated with the solution is given in figure 2. The flow is accelerated by the pressure gradient imposed through the streamwise boundary conditions until it reaches the reaction zone, whereupon the gradient flattens due to the heat release. We note that the pressure field exhibits none of the spurious effects associated with other characteristics based approaches, and that the dynamic pressure range (about $5N/m^2$) is consistent with that estimated from the velocity field using

$$\Delta p \sim \frac{1}{2}\Delta\left(\rho \mathbf{u}\cdot\mathbf{u}\right).$$

A solution cannot be obtained for this configuration using the LODI/NSCBC approach of Poinsot et al.

No asymptotic solutions for the curved flame configuration are available for benchmarking. Nevertheless, we may compare the curved flame structure to an analytic one dimensional solution [25], and assess whether the differences between the two are consistent with the effects driven by the local flow field. Figure 3 compares the progress variable profile of both flame structures along the centreline of the domain. The first curve is that obtained from the numerical solution, and contains transverse strain components as well as curvature. The second curve has been obtained from a one dimensional laminar flame simulation and has been verified via asymptotic methods. The flame in the curved, strained case is thinner than the one dimensional solution. This can be explained by comparing the normal strain rate ($= \partial u/\partial x$) encountered by the flame along the centre line of the solution. In figure 4, the curved flame is associated with a double peaked positive normal strain rate, the maximum magnitude of which is significantly less than that associated with the one dimensional flame profile. In the latter case, the higher positive strain rate acts to stretch the flame, and so produce the observed thicker flame profile. We conclude that the solution yields figures consistent with approximate estimates for the flow, although further analysis will be required to verify this.

4 Conclusions and future work

In this paper, we have presented a general method designed to prescribe time dependent boundary conditions. The new method is quite general, can be applied to multidimensional flows both with and without chemical reaction.

The scheme is based on a linearization of the solution about an appropriately defined base flow. This base flow is solenoidal in cold, low Mach number flows, but is non-zero in the presence of reaction and transport effects. The resulting formulation allows a wide class of boundary conditions to be applied, while still retaining acoustic transparency. The behaviour of the new approach shows a significant improvement over other methods.

The method is based on the calculation of the numerical divergence, and on the separation of inertial and acoustic effects. Consequently, the approach relies heavily on the numerical discretization schemes employed in the simulation. Future work will examine more thoroughly the interplay between the numerics and the boundary conditions, in particular examining the treatment of corners (which often have to contend with doubly poor numerical approximations). Additionally, more analysis will be undertaken to verify that the proposed boundary conditions are stable, using the energy estimates of Dutt [26]; the current simulations have shown themselves to be stable over very long simulation times (of the order of tens of thousands of time steps), but additional theoretical work is still required.

References

[1] F. Grinstein, Open Boundary Conditions in the Simulation of Subsonic Turbulent Shear Flows, J. Comput. Phys. 115 (1994) 43–55.

[2] S. Tsynkov, Numerical solution of problems on unbounded domains. A review, Appl. Numer. Math. 27 (1998) 465–532.

[3] K. Thompson, Time Dependent Boundary Conditions for Hyperbolic Systems, J. Comp. Phys. 68 (1987) 1–24.

[4] R. Vichnevetsky, Invariance Theorems Concerning Reflection at Numerical Boundaries, J. Comput. Phys 63 (1986) 268–282.

[5] G. Hedstrom, Nonreflecting Boundary Conditions for Nonlinear Hyperbolic Systems, J. Comp. Phys. 30 (1979) 222–237.

[6] D. Rudy, J. Strikwerda, Boundary Conditions for Subsonic Compressible Navier-Stokes Calculations, Comput. Fluids. 9 (1981) 327–338.

[7] D. Rudy, J. Strikwerda, A Nonreflecting Outflow Boundary Condition for Subsonic Navier-Stokes Calculations, J. Comp. Phys. 36 (1980) 55–70.

[8] T. Poinsot, S. Lele, Boundary Conditions for Direct Simulations of Compressible Viscous Flows, J. Comp. Phys 101 (1992) 104–129.

[9] F. Nicoud, Defining Wave Amplitude in Characteristic Boundary Conditions , J. Comp. Phys. 149 (1999) 418–422.

[10] M. Baum, T. Poinsot, D. Thévenin, Accurate Boundary Conditions for Multicomponent Reactive Flows, J. Comp. Phys. 116 (1994) 247–261.

[11] D. Thevénin, M. Baum, T. Poinsot (Eds.), Direct Numerical Simulation for Turbulent Reacting Flows , Editions Technip, Paris, 1996.

[12] J. Sutherland, C. Kennedy, Improved boundary conditions for viscous, reacting, compressible Flows , J. Comp. Phys. 191 (2003) 502–24.

[13] M. Giles, Nonreflecting boundary conditions for Euler equation calculations, AIAA J. 28 (1990) 2050–2058.

[14] T. Colonius, S. Lele, P. Moin, Boundary conditions for direct computation of aerodynamic sound generation, AIAA J. 31 (1993) 1574–1582.

[15] C. Rowley, T. Colonius, Discretely nonreflecting boundary conditions for linear hyperbolic systems, J. Comput. Phys. 157 (2000) 500–538.

[16] R. Prosser, Improved Boundary Conditions for the Direct Numerical Simulation of Turbulent Subsonic Flows I: Inviscid Flows, J. Comp. Phys. 207 (2005) 736–768.

[17] R. Prosser, Towards Improved Boundary Conditions for the DNS and LES of Turbulent Subsonic Flows Submitted to J. Comp. Phys.

[18] H. Yee, N. Sandham, M. Djomehri, Low-Dissipative High-Order Shock-Capturing Methods Using Characteristic-Based Filters, J. Comp. Phys. 150 (1999) 199–238.

[19] R. Klein, Semi-Implicit Extension of a Godunov-Type Scheme Based on Low Mach Number Asymptotics I: One Dimensional Flow, J. Comp. Phys. 121 (1995) 213 – 237.

[20] A. Majda, J. Sethian, The derivation and Numerical Solution of the Equations for Zero Mach Number Combustion, Combust. Sci. and Tech.. 42 (1985) 185–205.

[21] P. Roache, Quantification of Uncertainty in CFD, Ann. Rev. Fluid Mech. 29 (1997) 123–160.

[22] P. Roache, Verification of Codes and Calculations, AIAA J. 36 (1998) 696–702.

[23] A. Wray, Minimal Storage Time-Advancement Schemes for Spectral Methods, NASA Ames Research Center (1990).

[24] T. Echekki, J. Chen, Unsteady Strain Rate and Curvature Effects in Turbulent Premixed Methane-Air Flames, Combustion and Flame 106 (1996) 184–202.

[25] F. Williams, Combustion Theory - Second Edition, Addison Wesley, Menlo Park, California, 1985.

[26] P. Dutt, Stable Boundary Conditions and Difference Schemes for Navier-Stokes Equations, SIAM J. Num. Anal. 25 (1988) 245–267.

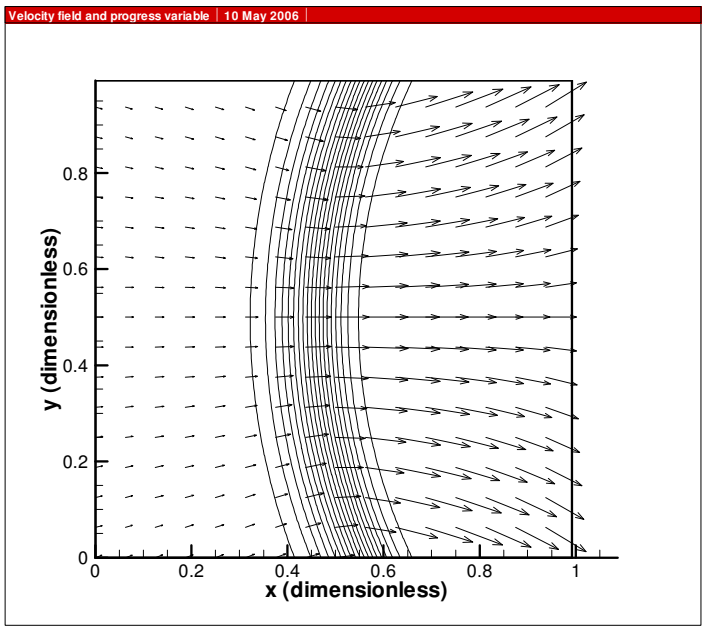


Fig. 1. Velocity field associated with curved reaction front.

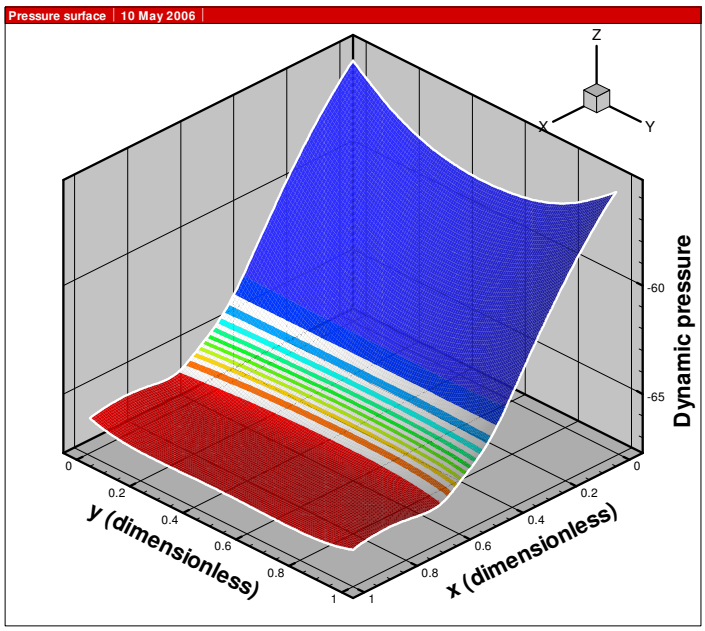


Fig. 2. Pressure surface coloured by progress variable. Contours striped to clarify flame structure.

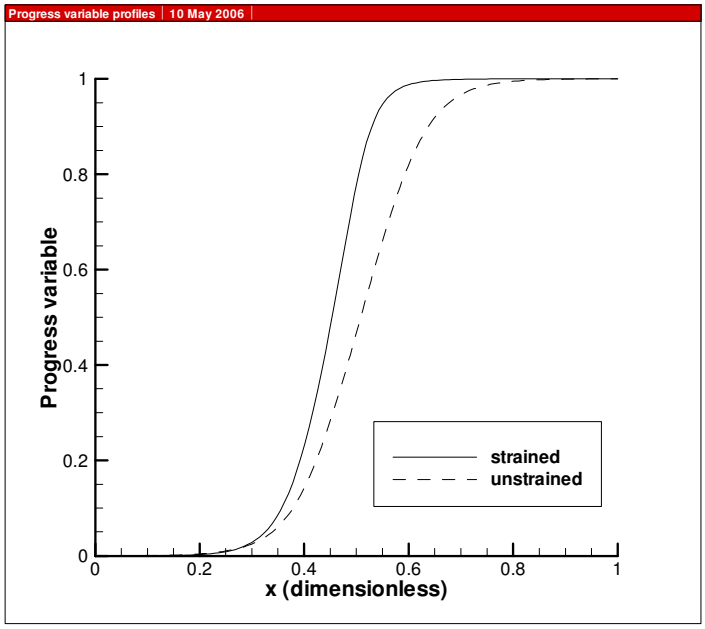


Fig. 3. Comparison of progress variable profiles in cases with and without transverse strain

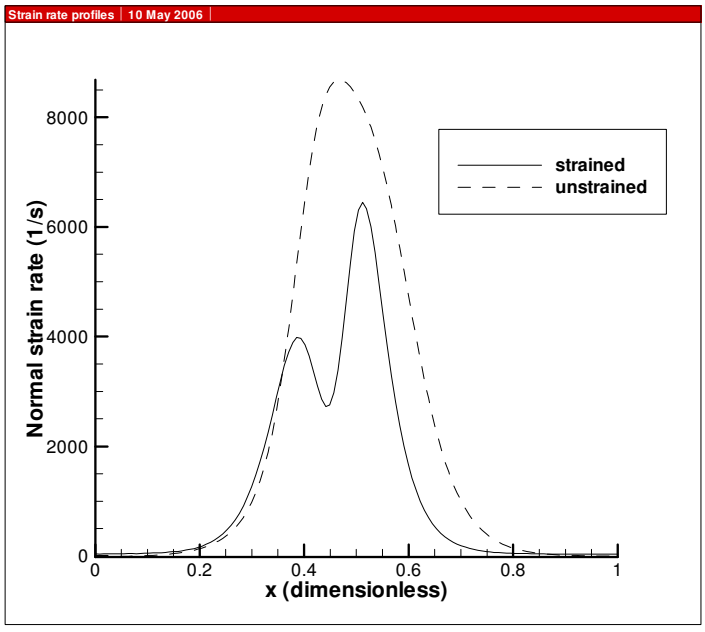


Fig. 4. Comparison of normal strain rates for one dimensional flame structure and curved flame structure.